# High quantum yield of the Egyptian blue family of infrared phosphors ($MCuSi_4O_{10}$, M = Ca, Sr, Ba)

Paul Berdahl, Simon K. Boocock, George C.-Y. Chan, Sharon S. Chen, Ronnen M. Levinson, and Michael A. Zalich

Citation: Journal of Applied Physics **123**, 193103 (2018); doi: 10.1063/1.5019808
View online: https://doi.org/10.1063/1.5019808
View Table of Contents: http://aip.scitation.org/toc/jap/123/19
Published by the American Institute of Physics



# High quantum yield of the Egyptian blue family of infrared phosphors ($MCuSi_4O_{10}$, M = Ca, Sr, Ba)

Paul Berdahl,[1,a)] Simon K. Boocock,[2] George C.-Y. Chan,[1] Sharon S. Chen,[1] Ronnen M. Levinson,[1] and Michael A. Zalich[3]
[1]*Heat Island Group, Lawrence Berkeley National Laboratory, Berkeley, California 94720, USA*
[2]*Shepherd Color Company, Cincinnati, Ohio 45246, USA*
[3]*PPG, Coatings Innovation Center, Allison Park, Pennsylvania 15101, USA*

(Received 17 December 2017; accepted 10 April 2018; published online 17 May 2018)

The alkaline earth copper tetra-silicates, blue pigments, are interesting infrared phosphors. The Ca, Sr, and Ba variants fluoresce in the near-infrared (NIR) at 909, 914, and 948 nm, respectively, with spectral widths on the order of 120 nm. The highest quantum yield $\phi$ reported thus far is ca. 10%. We use temperature measurements in sunlight to determine this parameter. The yield depends on the pigment loading (mass per unit area) $\omega$ with values approaching 100% as $\omega \to 0$ for the Ca and Sr variants. Although maximum quantum yield occurs near $\omega = 0$, maximum fluorescence occurs near $\omega = 70\,\mathrm{g\ m^{-2}}$, at which $\phi = 0.7$. The better samples show fluorescence decay times in the range of 130 to 160 $\mu$s. The absorbing impurity CuO is often present. Good phosphor performance requires long fluorescence decay times and *very* low levels of parasitic absorption. The strong fluorescence enhances prospects for energy applications such as cooling of sunlit surfaces (to reduce air conditioning requirements) and luminescent solar concentrators. *Published by AIP Publishing.*
https://doi.org/10.1063/1.5019808

## INTRODUCTION

Egyptian blue, $CaCuSi_4O_{10}$, and Han blue, $BaCuSi_4O_{10}$, have been utilized as important blue pigments for literally thousands of years.[1] The strontium variant, $SrCuSi_4O_{10}$, is less known but is a similar blue pigment.[2] In 2000, Pozza *et al.*[3] published photoluminescent spectra of Egyptian blue, Han blue, and Han purple ($BaCuSi_2O_6$), and proposed that photoluminescence could be used to distinguish between Egyptian and Han blue in ancient works of art. Accorsi *et al.*[4] provided more detailed information on the fluorescence of Egyptian blue and its application to artworks from ancient Egypt. The fluorescence emission spectra of the Ca and Sr compounds are very similar, whereas the Ba compound emits at slightly longer wavelength and with a broader spectrum. An important recent paper by Borisov *et al.*[5] displays excitation and emission spectra for the three compounds. For Egyptian blue, they also reported that the decay time $\tau$ is about 159 $\mu$s for their solid-state synthesized material. Grinding to reduce the particle size yields a shorter decay time of 126 $\mu$s, which they attributed to the introduction of defects by mechanical stress during grinding. This behavior is typical of phosphors.[6,7] Borisov *et al.* also found $\tau = 139$ $\mu$s for Kremer Pigmente's Egyptian blue, in agreement with the value to be reported here of 137 ($\pm 4$) $\mu$s.[5]

Applications of the near-infrared fluorescence of these blue compounds include optical chemosensors.[5,8] In these sensors, the excitation of two or more phosphors can produce fluorescent signals which when ratioed can be used to determine parameters such as pH. Biological labeling applications can be found in which the larger penetration depth of near-infrared vs. visible light is an advantage.[9] Near-infrared fluorescence also has application in optical electronics such as lasers.[10]

*Energy* applications of the alkaline earth copper silicate phosphors now look increasingly attractive due to their high quantum yield. The application that motivates the current research is energy conservation by reducing the temperature of sunlit objects. Current technology for this purpose relies on high near-infrared reflectance.[11] If an architect specifies blue or another dark color for a roof rather than white, the roof can be cooler in sunlight (saving air conditioning energy) if it efficiently rejects the invisible near-infrared sunlight component. This paper addresses the additional advantage gained if the roof also fluoresces in the deep red or near-infrared.[12] For luminescent solar concentrator (LSC) applications, a large thin transparent plate absorbs sunlight and then fluoresces near-infrared energy that eventually emerges from the edges of the plate for photovoltaic conversion to electricity.[13,14]

Long radiative lifetimes are desirable as they indicate the relative weakness of competing non-radiative relaxation mechanisms and therefore lead to higher quantum yield (efficiency) of the fluorescence process. However, long lifetimes are not sufficient for high quantum yield because parasitic absorption can lead to mere heating without fluorescence. Parasitic absorption can interfere with the excitation process and with the emission process. Thus, both the corresponding spectral ranges are important. For the specific impurity CuO, important for the present work, parasitic absorption occurs both in the excitation and in the emission spectra. If a parasitic impurity is added to (or not removed from) a fluorescent phosphor, we expect a diminished quantum yield but an unchanged decay time.

[a)]Author to whom correspondence should be addressed: paul.berdahl@gmail.com.

Measurements of fluorescence intensity can be used to determine the quantum yield of phosphors. However, the emitted light need not have a simple angular distribution, so an integrating sphere is needed to collect the fluorescence. Also, calibrated spectrometers are needed. Thus, complete quantum yield measurements are not convenient and are less available in the literature than fluorescence decay lifetimes. The method of de Mello *et al.*[15] has been employed. Based on this method, the quantum yield of Kremer Egyptian blue was reported as 10.5%.[4] For the Sr and Ba analogs fabricated by hydrothermal synthesis, quantum yields were found to be 8.5% and 6.9%, respectively.[16]

In this work, we use a novel method for the determination of quantum yield, namely, temperature measurements in full sunlight.[12] This approach is motivated by the "cool roof" application, in which we want to know how much the sunlit roof (or other facade) is cooled by its fluorescence. Test sample temperatures are compared in full sunlight with calibrated non-fluorescent gray samples, to determine the effective solar reflectance (ESR). Figure 1 illustrates the principle. Here, the sample under test is in the center, flanked by two calibrated samples on a thermally insulated support. The temperature rise in full sun is determined by the balance between solar heating and the cooling effects of fluorescence, longwave emission, and convection to the ambient air. The absolute values of the temperature vary with wind speed, but the performance of the fluorescent blue sample can still be determined by comparison with the calibrated non-fluorescent samples.

The solar reflectance (SR) is determined in the usual way based on spectral solar reflectance (excluding fluorescence) and a standard solar spectrum. The difference ESR – SR represents the fluorescence contribution to the ESR. From this contribution and by knowing the spectrum of the fluorescence, we can determine the number of photons emitted. The number of incident solar photons absorbed in the excitation spectral range is determined from the spectral reflectance. Finally, the quantum yield is the ratio of fluoresced to absorbed numbers of photons. We find that the pigment loading $\omega$ (pigment mass per unit area, in g m$^{-2}$) affects the quantum yield $\phi$ with larger concentrations having lower $\phi$; this effect is attributed primarily to parasitic absorption. Peak values of the quantum yield thus occur at low values of $\omega$, below 10 g m$^{-2}$. On the other hand, for a given amount of excitation radiation, peak values of fluorescence occur for $\omega$ in the range of 20 to 100 g m$^{-2}$, with the larger values corresponding to situations in which parasitic absorption is less important.

## EXPERIMENTAL AND THEORETICAL DETAILS

### Synthesis

The barium and strontium copper silicate blue pigments were synthesized at Shepherd Color using traditional ceramic techniques. Starting raw materials, in appropriate proportions, were mixed together intimately using intensive dry blending. The dry mixtures were homogenized by screening through fine brass cloth mesh, and then administered to ceramic crucibles for firing. As a source of alkaline-earth, the corresponding carbonate was used, barium or strontium as appropriate. For copper, finely ground copper (II) oxide was chosen, while silica was furnished as finely ground amorphous silica, free of alkali. Lanthanum was introduced as the lanthanum (III) carbonate and was always accompanied by an equimolar amount of lithium carbonate to maintain charge balance.[17]

All pigments were built to a parent stoichiometry of $M(\mathrm{Cu})\mathrm{Si_4O_{10}}$, or $M_y(\mathrm{La})_x(\mathrm{Li})_x(\mathrm{Cu})_y\mathrm{Si_4O_{10}}$, where $M$ is either Ba or Sr, and the coefficients $x$ and $y$ sum to unity. The mixed powders were calcined in air at 850 °C, with a soak no shorter than 5 h. The resulting fired products were coarsely ground in a mortar and pestle, then fine ground once on a jet-mill, or wet-ground with fine zirconia beads in de-ionized water to a tractable size.

Elemental composition was determined by x-ray fluorescence, which found levels of all elements (excepting lithium and oxygen) to be consistent with the target compositions.

The crystal phase of each finished pigment was confirmed by x-ray powder diffraction in reference to patterns for parent phases found in the ICDD (International Centre for Diffraction Data) PDF-4+ database. The barium copper tetra silicate, with equimolar lanthanum and lithium substitution for copper and barium, reported as Effenbergerite, $\mathrm{BaCuSi_4O_{10}}$, has powder pattern 04-007-5484. The unsubstituted strontium copper

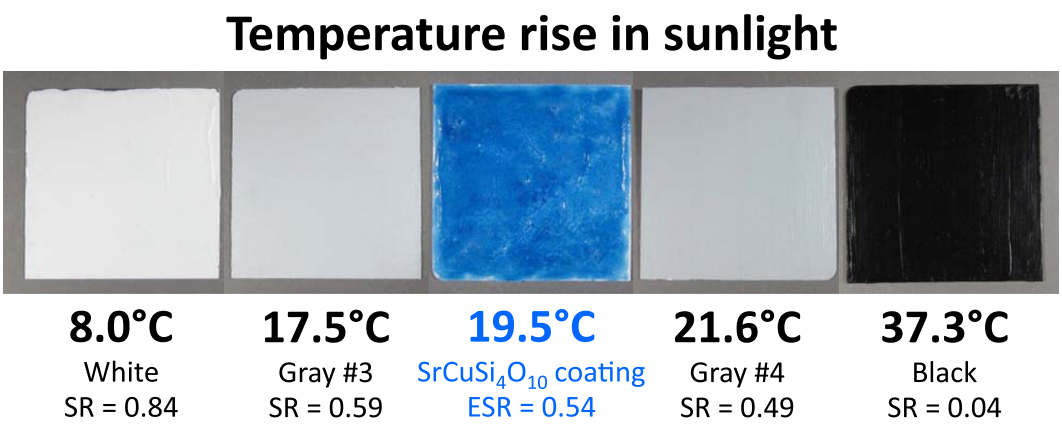


FIG. 1. Temperature rise above air temperature observed in full sun for five samples, each 75 mm square. The white and black samples show low and high temperatures. The ESR is determined by interpolation from the calibrated samples adjacent to the blue coating under test.

silicate analog to Han blue was reported as Wesselsite, pattern 04-009-5401. The median particle sizes of the barium and the strontium compound powders were 1.3 and 49 $\mu$m, respectively.

The X-ray diffraction measurement for the barium copper silicate doped with lanthanum and lithium is shown in Fig. 2(a) and the corresponding data of the strontium copper silicate are shown in Fig. 2(b). The pattern of Tenorite (CuO) code amcsd 0018812 (amcsd stands for American Mineralogical Crystal Structure Database) is also shown, as this impurity is black and is often present in these compounds. Here, the barium compound shows no evidence for CuO, while the strontium compound contains a trace (peak at 35.5°).

## Instrumentation

Fluorescence measurements, conducted at Lawrence Berkeley National Laboratory (Berkeley Lab), used a compact Ocean Optics S2000 spectrometer fitted with a 150 mm Labsphere integrating sphere. (We use the term fluorescence as a general synonym for photoluminescence and avoid the term phosphorescence.) The light source is a tungsten incandescent lamp with xenon gas fill. The incident light is directed through a port on the top of the integrating sphere onto the sample at a port on the bottom of the sphere. A 725 nm short-pass filter with optical density 4 (attenuation better than $10^{-4}$ in the stop band) blocks excitation light that would otherwise overlap with the fluorescence spectrum. The spectrometer receives light from the integrating sphere by means of an optical fiber and uses a diffraction grating to disperse the spectrum on a silicon array detector. The silicon detector covers a spectral range of about 500–1100 nm.

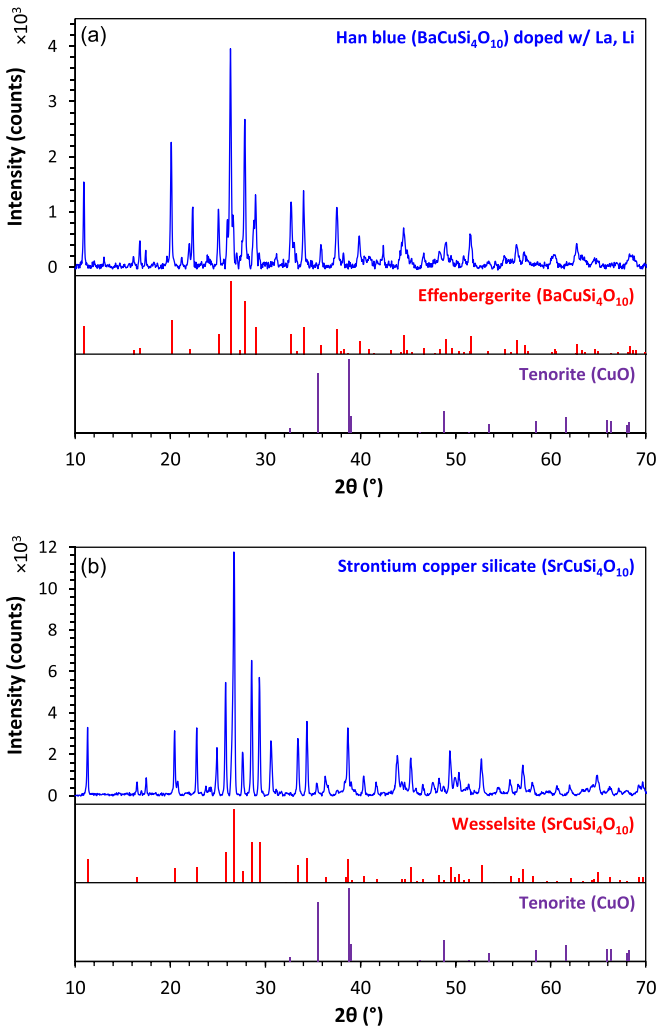


FIG. 2. (a) X-ray powder diffraction of the $BaCuSi_4O_{10}$ sample doped with La and Li. The pattern matches Effenbergerite (amcsd 0013767). (b) X-ray powder diffraction pattern of $SrCuSi_4O_{10}$. The pattern matches Wesselsite (amcsd 0013766).

Pulsed fluorescence measurements used an in-house fabricated pulse generator to drive three red light emitting diodes (620 nm) each with 1 A, 10 $\mu$s pulses with ~1 ms pulse repetition interval. The fluoresced light was passed through a 695 nm long-pass filter and focused onto a Thorlabs DET 200 fast (ns) photodiode. The photodiode output was processed by an SRS 570 low noise current preamplifier and then acquired by a Tektronix 3054 digital oscilloscope. The 1/$e$ response time of the whole detection system is approximately 3.4 $\mu$s.

Diffuse spectral reflectance measurements were made with a Perkin-Elmer Lambda 900 UV-VIS-NIR spectrometer fitted with a 150 mm Labsphere integrating sphere. A photomultiplier tube serves as a detector from 250 to 860 nm; at longer wavelengths up to 2500 nm, a PbS photoconductive detector is employed. The standard solar spectral irradiance used to compute solar averages (AM1GH, air-mass 1 global horizontal) represents the radiation received by a horizontal surface with the sun overhead on a clear day, summing to 1090 W $m^{-2}$.[18]

## Sample preparation

Phosphor powders are useful for screening materials. However, loose powders can introduce variability in repeated experiments depending on how the powder is packed or otherwise arranged. Powders suspended (dispersed) into a coating offer the advantage of durability, and reference samples can be used repeatedly. The phosphors have a tetragonal structure with refractive indices of 1.63 (ordinary ray, electric field perpendicular to the $c$-axis) and 1.59 (extraordinary ray).[2,19,20] Since the acrylic polymer has an index of ~1.5, scattering is reduced relative to a powder in air, and the color is a darker blue. All the pigmented coating samples used in the current work were prepared at Berkeley Lab by hand-dispersing pigments into a transparent acrylic base (Liquitex gloss medium and varnish) with a spatula, which does not lead to an ideal dispersion. These coatings crack upon drying (and are patched to fill cracks), and do not resemble commercial coatings. Coatings are applied with a spatula over a white substrate which is itself composed of three brushed layers of an acrylic artist's white coating (total dry film thickness about 150 $\mu$m) on an aluminum panel. This white substrate has a reflectance of ~0.9 from 500 to 1000 nm and serves to reflect excitation radiation that passes through the test coating, enhancing absorption by the phosphor. Additionally, the diffuse fluoresced emission is directed outward from the coating by the white substrate.

### Theoretical considerations

It would be useful to have a complete numerical radiative transfer model for phosphor particles suspended in a medium above a white or black substrate. However, modeling the radiative performance of even non-fluorescent coatings is complex.[21,22] If the incident light is collimated, one needs to keep track of how the diffuse radiation field develops due to scattering. One also needs to know the differential scattering cross section of the particles. The treatment of scattering needs to be approximated unless complete solutions of the Boltzmann-type photon transport equation are to be found. Furthermore, there are interface reflectances that depend on the photon incidence angle and polarization; total internal reflection at the top interface is particularly important. Such a code is certainly achievable, but we leave this problem to others. We resort to qualitative and semi-quantitative analysis supported by experimental data.

Consider a thin phosphor-pigmented layer (coating) supported by either a white or black substrate, illuminated with excitation radiation by a beam at normal incidence, as illustrated in Fig. 3. Here, thin means that the phosphor only absorbs a small fraction of the incident radiation. Also, for simplicity, assume that the black and white layers are perfect, with reflectances of 0 and 1. Scattering by the phosphor is neglected. If the absorption coefficient (with units of inverse length) is $\alpha$ and the layer thickness $h$, then the fraction of incident radiation absorbed by the black-backed layer is $\alpha\, h$. For the white-backed layer, additional absorption is caused by the diffusely reflected radiation. As an approximation, the typical path length of the reflected radiation is increased by a factor of two. (The factor of two is exact in the limit $\alpha\, h \to 0$, but slightly smaller factors will apply in realistic situations.) Thus, the total absorbed fraction of the white-backed layer is roughly $3\ \alpha\, h$. Even this value is an underestimate, due to the large reflectance for diffuse radiation ($\sim$0.6) at the underside of the top interface, a consequence of total internal reflection.[21]

Almost all of the fluoresced radiation emerges from the white-backed layer, whereas only about one fifth of the radiation emerges from the black-backed layer. (Of the upward-emitted radiation, only 2/5 is transmitted by the upper interface.) Therefore, we expect the white-backed layer to fluoresce with about 15 times the intensity of the black-backed layer. In one experiment, with a coating containing 12 g m$^{-2}$ of strontium copper silicate ($SrCuSi_4O_{10}$) phosphor on a microscope slide, we found that the fluorescence intensity with a white surface below the slide was like that of a coating applied directly to a white substrate. Replacing the white surface below the slide with black electrical tape adhered underneath the slide yielded a fluorescence intensity that was smaller by a factor of 17. Thus, a reflective underlayer greatly enhances fluorescence.

As already mentioned, long fluorescence decay times are desired. From the literature on phosphors generally,[6,7] and from the study by Borisov *et al.*,[5] we note that larger crystalline particles, free from deleterious impurities, strain, and other defects, are desirable. If small particles must be produced by grinding, reducing the decay time, post annealing may be helpful. Long decay times are indicative of the weakness of deleterious non-radiative relaxation processes

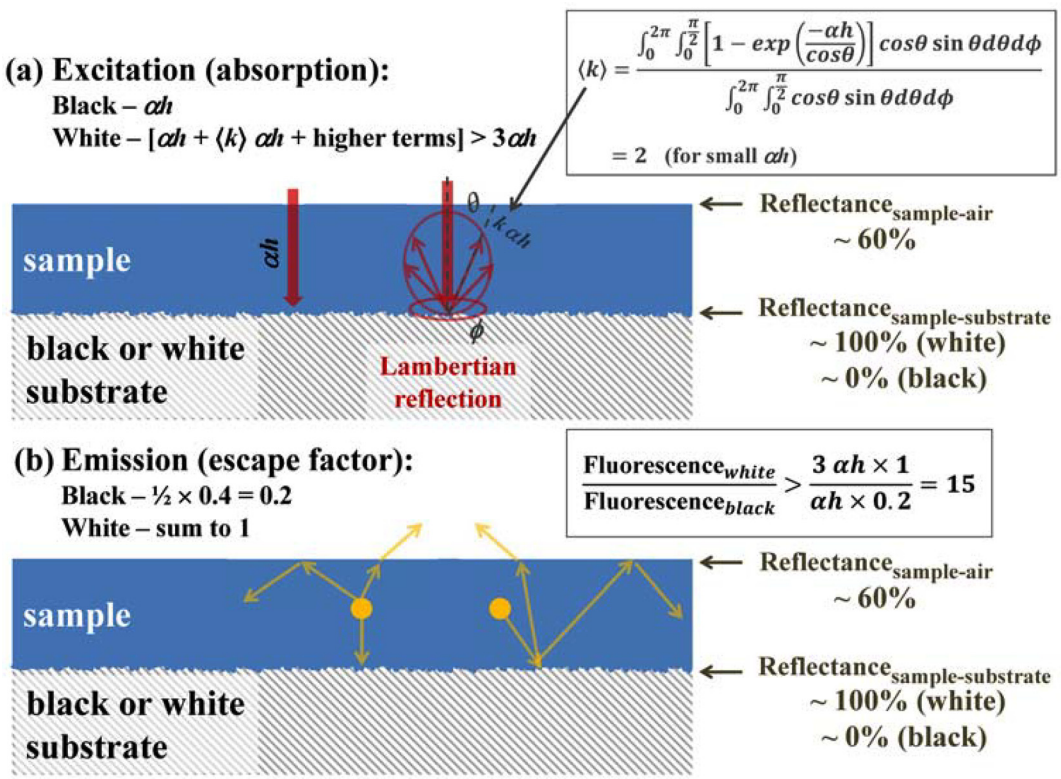


FIG. 3. Schematic depiction of radiation transport in thin blue fluorescent coatings over ideal white or black substrates. (a) Absorption of normally incident excitation radiation. (b) Emission of near-infrared fluorescence.

and are required for high quantum yields. Of course, parasitic absorption can interfere with high quantum yields, but it is helpful that long decay times can be measured even in the presence of parasitic absorption.

### Determination of quantum yield

In classical measurements of quantum yield, one wavelength near the center of the excitation range is used and the emission spectrum is integrated to determine the number of emitted photons. In the case at hand, the total emitted energy is determined from the ESR (effective solar reflectance) calorimetric measurement of temperature in sunlight. The fluorescence contribution to the ESR is then determined by subtracting the conventional spectrometer-measured SR (solar reflectance). (In general, the conventional SR measurement may require filters to exclude fluorescence,[11] but in this paper they are not needed.) The spectrum of emission is determined separately. Since the spectral distribution is known, the emitted photon flux can be determined from the energy flux.

Accounting for the number of excitation photons absorbed is more subtle. The spectral absorptance $A$ of a sample is compared with that of a sample with no pigment, $A_o$. If the coating layer is optically thin, then the absorptance of the pigment can be approximated by $A - A_o$. If, on the other hand, the layer is optically thick, with $A$ approaching unity, then the absorption of the substrate is nearly zero. With acceptable accuracy for our problem, in which $A_o$ is small, we perform a linear interpolation for $A'$, the pigment absorption, as

$$A' = (A - A_o)/(1 - A_o). \quad (1)$$

Thus, $A' = 0$ when $A = A_o$, and $A' = 1$ when $A = 1$. For the integration over wavelength, we multiply by the spectral photon flux of our standard solar spectrum and, for convenience, take the ends of the excitation spectrum as the points at which the excitation strength falls to 5% of its peak value, based on the spectra shown by Borisov *et al.*[5]

Also, we wish to determine the fraction of the fluoresced photons which are absorbed by the substrate with $A_o = 0.1$ rather than emitted by the layer. If $A_o$ were zero, this fraction would be 0%. For a downward-directed photon, the absorption probability is approximately $A_o$. Such a photon may be reflected several times between the white substrate and the coating top; the resulting absorption probability is nevertheless $A_o$. An upward-directed photon is either transmitted by the top interface, with 40% probability, or reflected with 60% probability. On being reflected, it is now downward directed and consequently has probability $A_o$ for absorption. Summing the possible outcomes, we find that the overall probability of absorption is 0.8 $A_o$. Thus, we conclude that 8% of the fluoresced photons are absorbed by the imperfect white substrate.

The state of the art of ESR measurements is still not very well developed; however, work is being conducted to improve the technique.[23] This latest technique uses a rotating sample stage to ensure that identical specimens will attain equal temperatures. The basic measurement difficulty is temperature fluctuation caused by wind. Convective heat transfer is temporally and spatially irregular due to atmospheric turbulence. Measuring only during periods of low wind speed is helpful but not a panacea. The effective solar absorptance ESA = 1 – ESR tends to have errors on the order of 5% of ESA. Thus, for example, if ESA = 0.40 (ESR = 0.60), the uncertainty is roughly ±0.02. Now, the fluorescence contribution to ESR may be on the order of 0.10, or even smaller, so that the experimental error can be undesirably large. This difficulty is ameliorated by utilizing ESR measurements only in favorable circumstances. Most fluorescence measurements are performed on a relative basis, comparing unknown samples to a "bright" reference sample, which is in turn calibrated by the ESR technique.

## OPTICAL MEASUREMENTS

### Fluorescence

After a process of screening pigment powders[24] for bright near-infrared fluorescence, two promising materials were found to be $SrCuSi_4O_{10}$ and a variant[17] of Han blue ($BaCuSi_4O_{10}$) which is co-doped with La and Li. These pigments were synthesized by the solid-state reaction technique at Shepherd Color and initially screened at PPG. Selected samples were forwarded to Berkeley Lab for additional study.

Figure 4(a) shows fluorescence curves of five acrylic coatings pigmented with $SrCuSi_4O_{10}$ powder. The dips at 880 and 945 nm are merely artifacts of the spectrometer system. Furthermore, the silicon array detector has diminished sensitivity at longer wavelengths. Thus, the central wavelength in these spectra is a slightly less than 900 nm, whereas calibrated spectrometer measurements[5] find a nearly symmetrical broad peak at 914 nm. Despite the limitations of the spectrometer, one can see that progressing from low to high pigment concentration, the spectrum shifts slightly to longer wavelengths. One likely explanation is that the intrinsic absorption of the strontium copper silicate compound extends from shorter excitation wavelengths to the 880 nm region and thereby encroaches on the left side of the fluorescence spectrum. Additionally, we suggest that this red shift is partly due to small amounts of the black absorbing impurity CuO. CuO is a semiconductor with band edge in the 900 nm region which becomes less absorptive with increasing wavelength in the 900 nm region.[25,26] Stated another way, CuO selectively attenuates the shorter wavelengths and thereby causes a small red shift.

Figure 4(b) shows analogous fluorescence data, acquired as in Fig. 4(a), but for commercially available $CaCuSi_4O_{10}$ (Egyptian blue from Kremer). Clearly, the Egyptian blue pigment is less fluorescent than the Sr compound. However, Fig. 4(c) shows fluorescence data of Egyptian blue pigment that has been soaked in 0.3 M HCl for 12 h ("washed") to dissolve small amounts of CuO. The fluorescence of the purified Egyptian blue pigment is then quite comparable to that of $SrCuSi_4O_{10}$ (strontium copper silicate).

Decay time measurements are summarized in Fig. 5. The curves are normalized to unity at zero time, and then displaced vertically by 10% from one another for clarity.

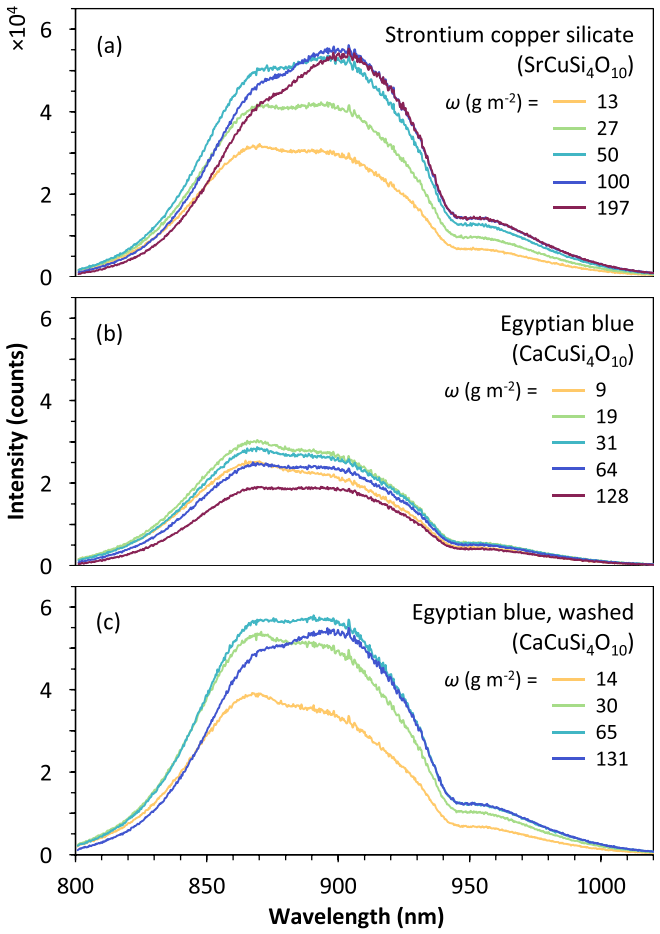


FIG. 4. Measured spectral fluorescence intensities of (a) five coatings pigmented with strontium copper silicate; (b) five coatings with commercial Egyptian blue pigment from Kremer Pigmente; and (c) four coatings with the same commercial Egyptian blue pigment that has been treated with HCl to reduce the amount of CuO. Each coating was applied to a white substrate.

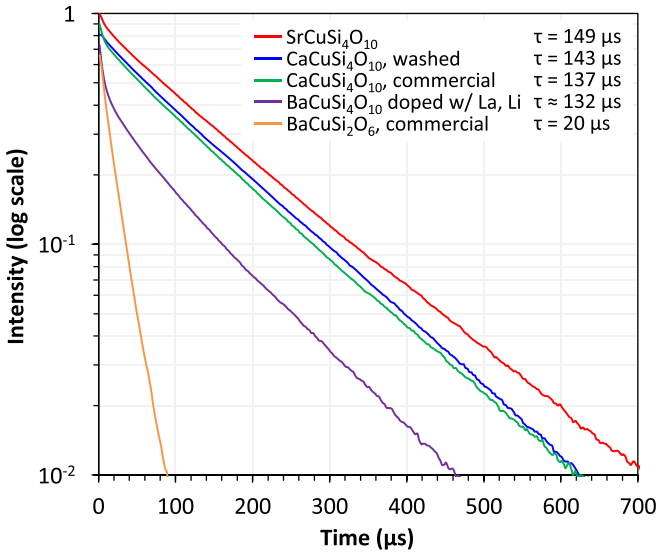


FIG. 5. Fluorescence decay curves. For the top three curves, the interval 25 to 300 $\mu$s was used to extract the time constant $\tau$. The Han blue (La, Li doped $BaCuSi_4O_{10}$) sample shows evidence of more than one decay; the longer decay was estimated based on the 125 to 400 $\mu$s period. For Han purple ($BaCuSi_2O_6$), the 25 to 100 $\mu$s interval was used.

The top three curves are linear on the logarithmic plots, for which the experimental uncertainties are about $\pm 4$ $\mu$s. The La and Li doped Han blue ($BaCuSi_4O_{10}$) data deviate from a straight line. One possible explanation is the presence of an additional, shorter time constant. It is tempting to think that it might contain some Han purple ($BaCuSi_2O_6$), as this has a short time constant of 20 $\mu$s. However, x-ray diffraction does not show this impurity. The Han purple sample is comparably bright with the other materials at $\sim$10 $\mu$s, but, due to its short time constant, the total number of photons is smaller by a factor of about seven. Our lifetime measurements are in good agreement with Fig. 5 of Ref. 5 for $SrCuSi_4O_{10}$ and for Egyptian blue. For Han blue, there are some differences which are understandable since our sample is doped with La and Li, and there is a lack of a simple exponential decay. The time constants of the original and washed Egyptian blue are very similar—equal within experimental uncertainty—even though the HCl washed sample exhibits much stronger fluorescence.

Comparisons with the literature indicate that samples synthesized by hydrothermal methods generally have a larger surface area and shorter decay time than those made by the solid-state reaction method. For example, Ref. 16 gives 16 and 33 $\mu$s for the Sr and Ba compounds, whereas Fig. 5 lists 149 and 132 $\mu$s. Also, for Han (Chinese) purple, Ref. 27 gives 6.4 $\mu$s, whereas we have obtained 20 $\mu$s for a commercial sample from Kremer. For Egyptian blue manufactured by Kremer, we have obtained 137 $\mu$s, which, as already mentioned, agrees well with that by Borisov *et al.*[5] Borisov *et al.* also found 159 $\mu$s for unground samples by solid-state reaction synthesis. Additional values reported for Egyptian blue by solid-state reaction synthesis are 107 $\mu$s,[4], 142 $\mu$s,[28] and about 160 $\mu$s.[29]

The fluorescence measurements presented in Fig. 4 are summarized in Fig. 6, which shows the area under each peak, relative to the area of the reference sample of $SrCuSi_4O_{10}$ with pigment loading $\omega = 100\,\mathrm{g\,m^{-2}}$. This reference sample has an effective solar reflectance (ESR) of 0.544, a spectrometer

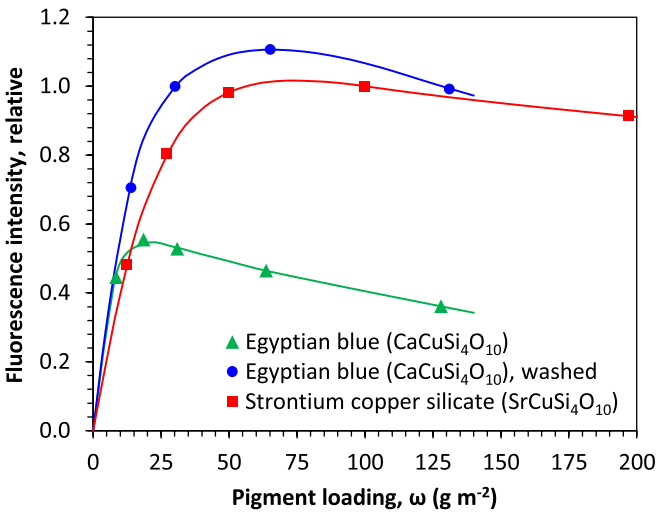


FIG. 6. Intensity of fluorescence, integrated over wavelength, as a function of pigment loading, based on the data in Fig. 4. The sample at $\omega = 100\,\mathrm{g\,m^{-2}}$ was used for reference and assigned the value 1.0.

determined solar reflectance (SR) of 0.410, and therefore a fluorescence contribution of 0.134. Given the 1,090 W $m^{-2}$ energy content of our reference solar spectrum, the fluorescence energy flux in full sun is 146 W $m^{-2}$. Furthermore, the central photon wavelength is 914 nm, which allows us to estimate the photon flux as $6.73 \times 10^{20}$ $m^{-2}$ $s^{-1}$. Now, we turn to the issue of determining the number of exciting photons that are absorbed.

### Spectral reflectance measurements

Figure 7(a) shows spectral reflectance data for the five samples presented in Fig. 4(a). The top curve represents a sample with no pigment, i.e., a transparent acrylic coating over a white substrate. Compared with the curves below, one can see that $SrCuSi_4O_{10}$ absorbs from about 475 to 880 nm, which is the excitation region. There is only weak absorption between 880 and 1100 nm. Reflectance data of Egyptian blue appear in Fig. 7(b) for the untreated pigment and Fig. 7(c) for the Egyptian blue pigment washed with HCl. The untreated Egyptian blue shows much more absorption in the 880 to 1100 nm region compared to the same washed pigment and the Sr pigment. It also shows less peak-to-valley variation in the visible region. Both characteristics can be attributed to parasitic absorption by CuO.

X-ray diffraction data in Fig. 8 of the as-received and washed Egyptian blue powders show small peaks at 35.5° due to CuO. The peak is smaller in the washed sample but still present. The optical reflectance data of Figs. 7(b) and 7(c) are consistent: the parasitic absorption in the 880 to 1100 nm region is reduced but not eliminated by washing. The visible region reflectance indicates that all samples are blue as shown in the insets, with high blue reflectance (400 to 500 nm) and low reflectance in the 500 to 700 nm region. The peak-to-valley distance of the untreated Egyptian blue is enhanced by the reduction of the CuO impurity.

The rate of photon absorption by the pigments is computed from the reflectance curves with and without pigments shown in Fig. 7. As detailed earlier, the absorptance attributed to the substrate is reduced to account for photons absorbed by the pigment. The excitation region is taken to be 475 to 880 nm; photons outside this range are assumed not to excite the pigment. Figure 9 summarizes the rate of photon absorption.

### Quantum yield

The quantum yield is now readily computed and is displayed in Fig. 10. Most notably, the quantum yield $\phi$ varies with the pigment loading $\omega$ (mass per unit area) and, for small $\omega$, approaches unity for the $SrCuSi_4O_{10}$ and $CaCuSi_4O_{10}$ compounds. Due to the limited measurement accuracy of the ESR measurement for the 100 g $m^{-2}$ $SrCuSi_4O_{10}$ calibration sample, the values of $\phi$ are uncertain by ca. ± 20%. Nevertheless, the trends and overall high values are clear. Figure 6 shows that the fluorescence is maximum near 70 g $m^{-2}$ for the better Sr and Ca compounds. Figure 10 then shows that at that maximum the quantum yield is ca. 0.70 (±0.15). It seems likely that if the impurity concentration of CuO can be further reduced, even higher performance may be feasible.

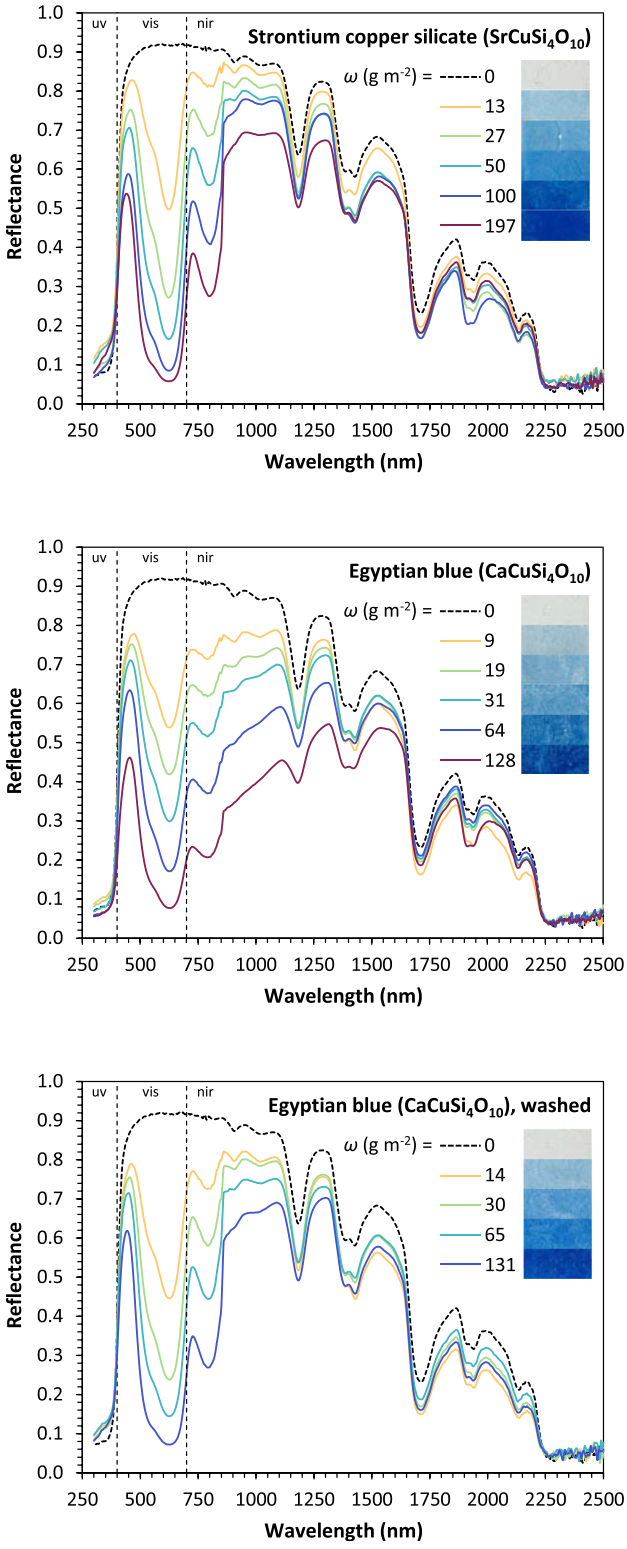


FIG. 7. (a) Measured spectral reflectance of the coatings of Fig. 4(a) and of one transparent coating with no pigment. The inset shows colors. (b) Spectral reflectance and images of the coatings of Fig. 4(b) (as received Egyptian blue). (c) Spectral reflectance and images of the coatings of Fig. 4(c) (Egyptian blue washed with HCl).

The quantum yield of the Han blue ($BaCuSi_4O_{10}$) compound doped with La and Li is based on a separate ESR measurement, subject to its own 20% uncertainty, but it seems

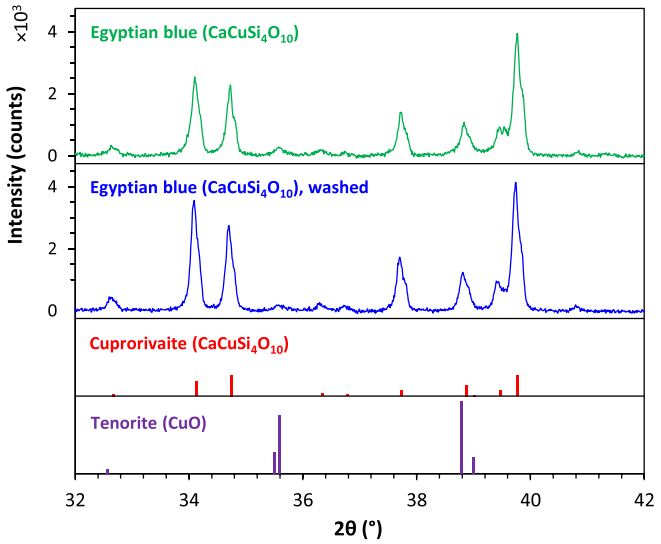


FIG. 8. X-ray diffraction data vs. scattering angle $2\theta$ for Egyptian blue, washed with HCl, and as received from Kremer. Both samples have some CuO (Tenorite, small peak at 35.5°), and there is less in the washed sample.

clear that this specific sample does not perform quite as well as its Sr and Ca counterparts.

In evaluating the quantum yield, we computed the number of excitation photons absorbed by the pigment, as distinct from the substrate. Also, we corrected for the fact that 8% of the fluoresced photons were absorbed by the imperfect white substrate.

## TWO ENERGY APPLICATIONS

### Cool roofing and facades

The efficient blue fluorescent pigments, calcium and strontium copper tetra-silicates, are suitable for fabricating blue-colored surfaces that stay cooler in the sun than non-fluorescent blues. The amount of fluorescent cooling can be more than 150 W $m^{-2}$ in full sun. Attention still must be paid to provide coating formulations that provide high near-infrared reflectance.

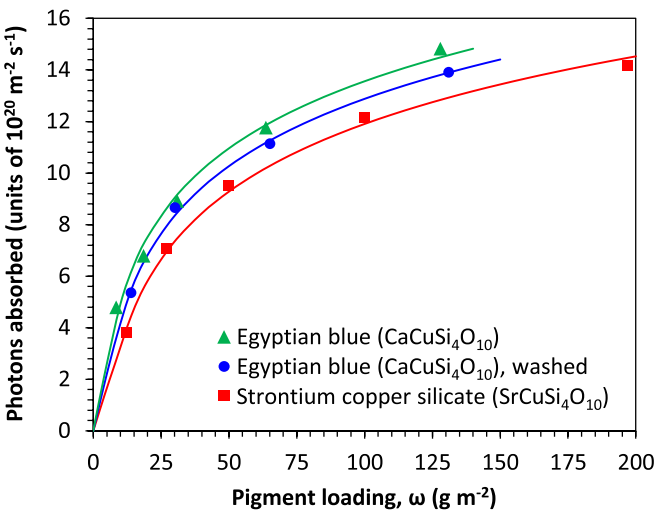


FIG. 9. Rate of photon absorption by the pigments between 475 and 880 nm in full sun computed from the spectral reflectance, the spectral reflectance of a sample with no pigment, and a standard solar spectrum.[18]

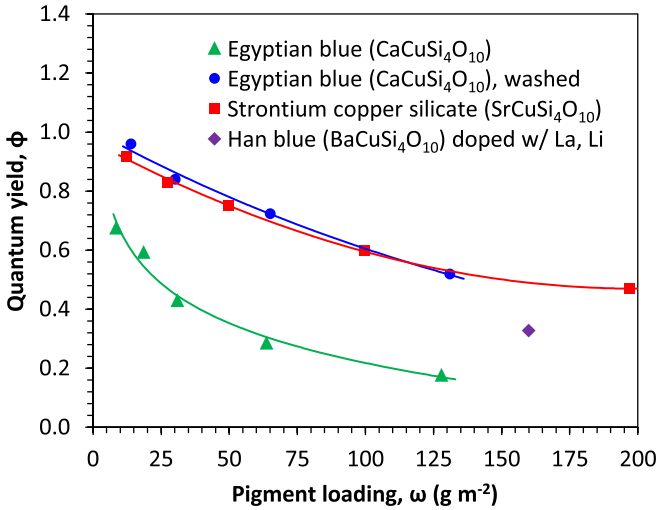


FIG. 10. The quantum yield of the pigmented coatings as a function of pigment loading (areal density), based on the data in Figs. 6 and 9. The single data point for the Han blue pigment is based on a separate ESR measurement, required by the longer wavelength of fluorescence.

For the ruby pigments studied earlier,[12] the use of colored co-pigments will reduce fluorescent performance because the excitation range covers the entire visible spectrum (except for the end of the red region in which fluorescence occurs). The currently investigated blue pigments do not absorb blue light. Consequently, a co-pigment can introduce absorption in the short wavelength part of the visible spectrum without impairing fluorescence. For example, a yellow co-pigment can be added to blue to provide a green color. Furthermore, an orange pigment can be added to obtain a cool black color.

Figure 11 shows four images of a coating with $SrCuSi_4O_{10}$ pigment by itself (blue), mixed with either of two yellow pigments to make green, and coated over orange to make a blue-shade black. Table I tabulates the performance of these samples.

Table II shows information on several additional samples that were characterized by ESR measurements. Of special note is the first sample with fluorescence contribution of 0.175, the largest value observed with the alkaline earth copper silicates. It utilized the washed Egyptian blue, with a nearly optimum pigment amount, and was very well dispersed. It absorbed and emitted about 17% more photons than the corresponding sample with $\omega = 65$ g $m^{-2}$ in Fig. 10, with the result that the quantum yield $\phi$ was the same, at 0.72.

If the yellow or orange co-pigments mentioned above can also fluoresce, an additional cooling effect can be obtained. For example, phosphors are used in some white LEDs to absorb blue light and emit yellow. One such compound is YAG:$Ce^{3+}$ ($Y_3Al_5O_{12}$:$Ce^{3+}$) which absorbs between 420 and 500 nm and emits between 500 and 650 nm.[30] Another possibility is a dye with similar absorption and emission properties. A dye would also minimize scattering. The use of such supplementary phosphors can further excite the alkaline earth copper silicate phosphor and enhance the NIR emission.

### Luminescent solar concentrators (LSC)

LSC devices utilize phosphors to absorb sunlight and emit fluorescence that can be trapped by total internal

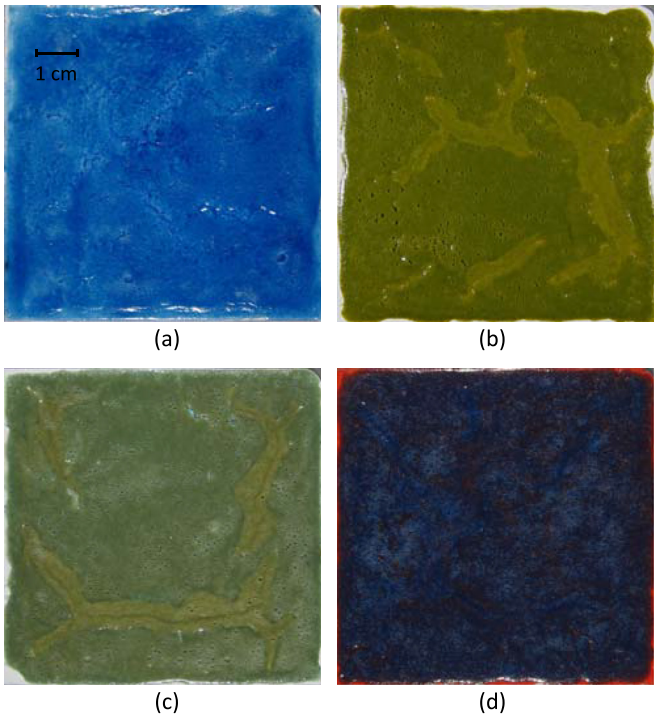


FIG. 11. Coating samples with the $SrCuSi_4O_{10}$ pigment with a bright white undercoating. (a) Blue pigment alone, (b) blue mixed with azo yellow (Diarylide yellow, PY83 HR70), and (c) blue mixed with Shepherd yellow 193 (A mixed oxide of Cr, Sb, Ti). Discoloration on green panels is caused by attempts to patch cracks that occurred during drying. (d) Coating sample, a blue-shade black in color, using the pigment over an orange coating, over white. The orange was Liquitex cadmium light red hue (imitation), one brushed coating. The spectrometer reflectance was 0.14 in the blue at 450 nm, 0.08 in the center of the visible (green) at 550 nm, and 0.10 in the red at 650 nm. Thus, this sample is nearly black.

reflection and delivered to photovoltaic cells positioned at the edges of a large plastic or glass sheet. The total area of expensive photovoltaic cells can thereby be minimized. While these devices have great potential, obstacles have delayed implementation. Part of the diffuse fluorescence is nearly normal to the sheet and therefore not trapped. In some designs, a selective dielectric interference filter helps confine the fluorescence. Absorption of the fluorescence can occur before it reaches the sheet edge. The Stokes shift is a double-edged sword: energy is lost due to the redshift of wavelength, but a large Stokes shift also reduces re-absorption

TABLE I. Optical and thermal performance of the four coatings with $SrCuSi_4O_{10}$ blue pigment shown in Fig. 11. The reflectance at 550 nm is included as an indication of visual brightness.

| Co-pigment | Fluorescent pigment loading ($g\ m^{-2}$) | Visual reflectance (550 nm) | Solar reflectance (SR) | Effective solar reflectance (ESR) | Fluorescence contribution (ESR-SR) |
|---|---|---|---|---|---|
| None | 100 | 0.17 | 0.410 | 0.544 | 0.134 |
| Shepherd 193 yellow | 90 | 0.23 | 0.384 | 0.507 | 0.123 |
| Azo yellow | 130 | 0.26 | 0.350 | 0.475 | 0.125 |
| Organic orange underlayer | 130 | 0.08 | 0.330 | 0.469 | 0.139 |

TABLE II. Five auxiliary samples for which optical and thermal performance data were obtained.

| Pigment(s) | Fluorescent pigment loading ($g\ m^{-2}$) | Visual reflectance (550 nm) | Solar reflectance (SR) | Effective solar reflectance (ESR) | Fluorescence contribution (ESR-SR) |
|---|---|---|---|---|---|
| Washed Egyptian blue (EB) | 68 | 0.15 | 0.394 | 0.569 | 0.175 |
| Washed EB, with organic orange underlayer | 60 | 0.06 | 0.263 | 0.388 | 0.126 |
| Washed EB, mixed with azo yellow | 128 | 0.16 | 0.196 | 0.304 | 0.108 |
| As received EB (not purified) | 128 | 0.14 | 0.268 | 0.360 | 0.092 |
| $Ba(La,Li)CuSi_4O_{10}$ | 160 | 0.19 | 0.363 | 0.438 | 0.075 |

losses. Finally, the quantum yield of the phosphor is important. Current reviews[14,31–33] indicate that an important class of prospective phosphors is organic dyes of which Ref. 14 gives 20 examples. Another class of phosphors is "quantum dots" such as nanoparticles of CdSe with shells of CdS that can absorb over an extended short-wave spectrum and emit fluorescence in a narrow long-wave band.[34] Other inorganic phosphors have not received close recent attention for LSC applications. Ruby, $Al_2O_3:Cr^{3+}$, is one possibility.[12,13,35] And now, with adequate quantum yield, the $MCuSi_4O_{10}$ (M = Ca, Sr, Ba) infrared phosphors should be investigated as well.

Li *et al.*[28] advocated the use of the Egyptian blue phosphor for LSC applications. They noted that performance declines only slightly at elevated temperatures and envisage that a polymer with nanoparticles or a specially formulated glass could host the blue particles in a transparent matrix with a matching refractive index. However, a maximum quantum yield of 10.5% is not acceptable for energy applications.[4] For various other applications such as temperature measurements using fluorescence, high efficiency is welcome, but not essential, provided the signal-to-noise ratio is acceptable. Our observation of quantum yields exceeding 70%, using these durable inorganic phosphors, may open a path for further LSC development.

## DISCUSSION

In view of the much smaller quantum yield based on the sparse measurements reported in the literature[4,16] for the alkaline earth copper tetra-silicates, and in view of the relative novelty of our procedure for measurements of this yield, we briefly review the technique. Instead of employing a single wavelength for excitation, we use natural sunlight. The spectral absorption of the phosphor is deduced from spectral reflectance measurements, as is the overall solar reflectance (excluding fluorescence). The determination of the fluorescence intensity is based on *temperature measurements in sunlight*, in comparison with calibrated non-fluorescent gray

reference samples. The difference between the effective solar reflectance determined from temperature measurements in sunlight and the ordinary spectrometer-determined solar reflectance gives the fraction of the incident solar flux which is re-radiated by fluorescence. (This fraction varies from 0.075 to 0.175 in Table II, for example.) Then, the number of fluoresced photons can be computed based on the known fluorescence spectrum. The quantum yield is thus an average over the components in sunlight that are absorbed by the phosphor.

The present technique for determining quantum yield using temperature measurements in sunlight has been employed once before.[12] The fluorescent pigment studied was ruby, the α-phase of $Al_2O_3$:Cr. For doping levels up to 3 wt. % $Cr_2O_3$, the quantum yield of coatings with ruby powder was found to be $0.83 \pm 0.10$. Some of the best work on this well-known material was done around the time of the demonstration of the first laser, see Maiman *et al.*[36] They studied a single crystal with light doping (0.05 wt. % $Cr_2O_3$) and found that the quantum efficiency varied with excitation wavelength in the range of 0.57–0.79. They concluded that the average value was $0.70 \pm 0.05$. Details preclude a precise comparison with that by Maiman *et al.*—single crystal vs. powder in a coating, anisotropy of ruby, dependence of emission spectrum with doping,[12] etc.—but their results provide evidence that measurements in sunlight can provide quantum yield values not greatly different from more traditional measurements.

A straightforward alternative approach to the determination of quantum yield could rely entirely on laboratory measurements using a lamp with a monochromator for excitation. After such measurements, the question would remain: what is the performance in the sun? The present approach merely answers this last question first, and then works backward to deduce what the quantum yield must be.

## CONCLUSION

Future applications of infrared fluorescence are enhanced by the high quantum yields of the alkaline earth copper tetra-silicates. It remains to be seen if the barium compound can match the very high performance of the calcium and strontium compounds.

Non-white coatings with high ESR (effective solar reflectance) are useful for energy conservation applications (e.g., to reduce air conditioning needs). Pigments used should have decay times $>140$ μs and contain as little CuO as possible. Coating systems should have a highly reflective backplane, optionally include near-infrared reflective pigments, and include a well-dispersed layer of the $MCuSi_4O_{10}$ (M = Ca, Sr, or Ba) near-infrared phosphor.

In addition to medium and dark blue colors, green and even black materials can be achieved by adding co-pigments. A blue-shade black with ESR exceeding 0.5 appears likely in the near term.

## ACKNOWLEDGMENTS

At Berkeley Lab, T. Kirchstetter and X. L. Mao provided advice and equipment. At PPG, initiation of the work was catalyzed by S. Hellring, J. Kulfan, C. Balliet, and I. Schwendeman, and ongoing support was provided by B. Kornish, J. Stalker, and M. Baxter. At Shepherd Color, W. Yuhasz and S. Davis synthesized samples of barium- and strontium-bearing alkaline-earth copper silicate blues and other IR-fluorescing pigments used for evaluation.

This work was supported by the Assistant Secretary for Energy Efficiency and Renewable Energy, Building Technologies Office of the U. S. Department of Energy under Contract Nos. DE-AC02-05CH11231 and DE-EE0006347. Support was also provided by the California Energy Commission under Agreement EPC-14-010.

[1]H. Berke, "The invention of blue and purple pigments in ancient times," Chem. Soc. Rev. **36**, 15–30 (2007).
[2]G. Giester and B. Rieck, "Wesselsite, $SrCu[Si_4O_{10}]$, a further new gillespite-group mineral from the Kalahari Manganese Field, South Africa," Miner. Mag. **60**, 795–798 (1996).
[3]G. Pozza, D. Ajò, G. Chiari, F. De Zuane, and M. Favaro, "Photoluminescence of the inorganic pigments Egyptian blue, Han blue and Han purple," J. Cult. Heritage **1**, 393–398 (2000).
[4]G. Accorsi, G. Verri, M. Bolognesi, N. Armaroli, C. Clementi, C. Miliani, and A. Romani, "The exceptional near-infrared luminescence properties of cuprorivaite (Egyptian blue)," Chem. Commun. **0**, 3392–3394 (2009).
[5]S. M. Borisov, C. Wurth, U. Resch-Genger, and I. Klimant, "New life of ancient pigments: Applications in high-performance optical sensing materials," Anal. Chem. **85**, 9371–9377 (2013).
[6]*Inorganic Phosphors: Composition, Preparation, and Optical Properties*, edited by W. M. Yen and M. J. Weber (CRC Press, 2004), p. 334.
[7]R. J. D. Tilley, *Colour and the Optical Properties of Materials* (John Wiley & Son, 2011), p. 378.
[8]C. McDonagh, C. S. Burke, and B. D. MaxCraith, "Optical chemical sensors," Chem. Rev. **108**, 400–422 (2008).
[9]M. H. V. Werts, R. H. Woudenberg, P. G. Emmerink, R. van Gassel, J. W. Hofstraat, and J. W. Verhoeven, "A near-infrared luminescent label based on $Yb^{III}$ ions and its application in a fluoroimmunoassay," Angew. Chem., Int. Ed. **39**(24), 4542–4544 (2000).
[10]S. Kuck, "Laser-related spectroscopy of ion-doped crystals for tunable solid-state lasers," Appl. Phys. B **72**, 515–562 (2001).
[11]R. Levinson, P. Berdahl, H. Akbari, W. Miller, I. Joedicke, J. Reily, Y. Suzuki, and M. Vondran, "Methods of creating solar-reflective nonwhite surfaces and their application to residential roofing materials," Sol. Energy Mater. Sol. Cells **91**, 304–314 (2007).
[12]P. Berdahl, S. S. Chen, H. Destaillats, T. W. Kirchstetter, R. M. Levinson, and M. A. Zalich, "Fluorescent cooling of objects exposed to sunlight – the ruby example," Sol. Energy Mater. Sol. Cells **157**, 312–317 (2016).
[13]P. S. Friedman and C. R. Parent, "Luminescent solar concentrator development," Project Report SERI/STR-211-3149 for the Solar Energy Research Institute, 1987.
[14]M. G. Devije and P. P. C. Verbunt, "Thirty years of luminescent solar concentrator research: Solar energy for the built environment," Adv. Energy Mater. **2**, 12–35 (2012).
[15]J. C. de Mello, H. F. Wittmann, and R. H. Friend, "An improved experimental determination of external photoluminescence quantum efficiency," Adv. Mater. **9**(3), 230–232 (1997).
[16]Y. Chen, M. Shang, X. Wu, and S. Feng, "Hydrothermal synthesis, hierarchical structures and properties of blue pigments $SrCuSi_4O_{10}$ and $BaCuSi_4O_{10}$," CrystEngComm **16**, 5418–5423 (2014).
[17]S. Jose and L. Reddy, "Lanthanum-strontium copper silicates as intense blue inorganic pigments with high near-infrared reflectance," Dyes Pigm. **98**, 540–546 (2013).
[18]R. Levinson, H. Akbari, and P. Berdahl, "Measuring solar reflectance – Part I: Defining a metric that accurately predicts solar heat gain," Sol. Energy **84**, 1717–1744 (2010).
[19]F. Mazzi and A. Pabst, "Reexamination of cuprorivaite," Am. Mineral. **47**, 409–411 (1962).
[20]G. Giester and B. Rieck, "Effenbergerite, $BaCu[Si_4O_{10}]$, a new mineral from the Kalahari manganese field, South Africa: Description and crystal structure," Mineral. Mag. **58**, 663–670 (1994).
[21]R. Levinson, P. Berdahl, and H. Akbari, "Solar spectral optical properties of pigments – Part I: Model for deriving scattering and absorption

coefficients from transmittance and reflectance measurements," Sol. Energy Mater. Sol. Cells **89**, 319–349 (2005).
[22]R. Levinson, P. Berdahl, and H. Akbari, "Solar spectral optical properties of pigments – Part II: Survey of common colorants," Sol. Energy Mater. Sol. Cells **89**, 351–389 (2005).
[23]R. Levinson, S. Chen, C. Ferrari, P. Berdahl, and J. Slack, "Methods and instrumentation to measure the effective solar reflectance of fluorescent cool surfaces," Energy Build. **152**, 752–765 (2017).
[24]M. Zalich and B. Kornish, "Fluorescent pigments for high-performance cool roofing and facades," Project Report Contract No. DE-EE0006347, 2016.
[25]*Handbook of Optical Constants of Solids*, edited by E. D. Palik (Academic Press, 1998).
[26]Q. Cheng, J. Chai, and Z. Zhang, "Investigation of double-layer coating with CuO particles of different concentrations on aesthetic and thermal aspects," Int. J. Therm. Sci. **105**, 36–44 (2016).
[27]Y. Chen, Y. Zhang, and S. Feng, "Hydrothermal synthesis and properties of pigments Chinese purple $BaCuSi_2O_6$ and dark blue $BaCu_2Si_2O_7$," Dyes Pigm. **105**, 167–173 (2014).
[28]Y. J. Li, S. Ye, C. H. Wang, X. M. Wang, and Q. Y. Zhang, "Temperature-dependent near-infrared emission of highly concentrated $Cu^{2+}$ in $CaCuSi_4O_{10}$ phosphor," J. Mater. Chem. C **2**, 10395–10402 (2014).
[29]Y. Zhuang and S. Tanabe, "Forward and back energy transfer between $Cu^{2+}$ and $Yb^{3+}$ in $Ca_{1-x}CuSi_4O_{10}$:$Yb_x$ crystals," J. Appl. Phys. **112**, 093521 (2012).
[30]Y. Kim, K. B. Shim, M. Wu, and H. K. Jung, "Monodispersed spherical YAG:$Ce^{3+}$ phosphor particles by one-pot synthesis," J. Alloys Compd. **693**, 40–47 (2017).
[31]W. G. H. M. van Sark, "Luminescent solar concentrators – A low cost alternative," Renewable Energy **49**, 207–210 (2013).
[32]M. K. Assadi, H. Hanaei, N. M. Mohamed, S. B. Saidur, R. Bashiri, and M. Moayedfar, "Enhancing the efficiency of luminescent solar concentrators (LSCs)," Appl. Phys. A **122**, 821 (2016).
[33]C. Tummeltshammer, A. Taylor, A. J. Kenyon, and I. Papakonstantinou, "Losses in luminescent solar concentrators unveiled," Sol. Energy Mater. Sol. Cells **144**, 40–47 (2016).
[34]N. D. Bronstein, Y. Yao, L. Xu, E. O'Brien, A. S. Powers, V. E. Ferry, A. P. Alivisatos, and R. G. Nuzzo, "Quantum dot luminescent concentrator cavity exhibiting 30-fold concentration," ACS Photonics **2**, 1576–1583 (2015).
[35]H. J. Hovel, R. T. Hodgson, and J. M. Woodall, "The effect of fluorescent wavelength shifting on solar cell spectral response," Sol. Energy Mater. **2**, 19–29 (1979).
[36]T. H. Maiman, R. H. Hoskins, I. J. D'Haenens, C. K. Asawa, and V. Evtuhov, "Stimulated optical emission in fluorescent solids. II. Spectroscopy and stimulated emission in ruby," Phys. Rev. **123**, 1151–1157 (1961).